

# Implementation of DBSCAN Method in Star Trackers to Improve Image Segmentation in Heavy Noise Conditions

Nevsan Şengil 

Department of Astronautical Engineering, University of Turkish Aeronautical Association, Ankara, Turkey

**Cite this article as:** N. Sengil, "Implementation of DBSCAN method in star trackers to improve image segmentation in heavy noise conditions," *Electrica*, 23(1), 3-10, 2023.

## ABSTRACT

Star trackers are currently the most accurate sensors for determining the attitude of a spacecraft. These sensors comprise not only highly capable optical detectors and processor units but also complicated software solvers. One of the main solvers employed in star trackers is image segmentation. In this study, the aim is to develop a hybrid image segmentation method which is a combination of both global thresholding and density-based spatial clustering of applications with noise (DBSCAN) method to increase detection probability of the stars in heavy noise. Secondly, a sorting algorithm is added to list the detected stars in terms of their brightness to increase the efficiency of the star tracking algorithm. Then, this new approach and two different conventional segmentation methods are applied to the Orion star constellation image polluted with Gaussian, salt and pepper, and uneven background noises. The resulting images of these segmentation methods are compared in terms of denoising capabilities. Although computationally more expensive, the proposed DBSCAN-based hybrid method displays a background pixel recovery performance of 99.5%, compared to Otsu global thresholding and adaptive thresholding methods' 73.5% and 79.9% recovery values, respectively. Additionally, it has been demonstrated that the sorting algorithm successfully listed the detected stars in accordance with their brightness.

**Index Terms**—DBSCAN, Gaussian noise, image segmentation, salt and pepper noise, star tracker, stray light.

## I. INTRODUCTION

Among the different types of attitude determination units such as sun sensors, magnetic sensors, Earth sensors, and horizon sensors, star trackers are the most accurate sensors used in spacecraft. Precise attitude information is required to orient directions of main or auxiliary thrusters, transmitting or receiving antennas, remote sensing sensors, and scientific payloads such as space telescopes. Star trackers comprise two fundamental units. These are a digital camera and a processor unit. These two units work together and sequentially perform image segmentation, star centroiding, star identification, and spacecraft attitude determination tasks. Naturally, the success of the image segmentation operation has an impact on the remaining algorithms.

The image segmentation performance is adversely affected by sensor-specific noise sources such as dark current noise, photon shot noise, and switching noise in the form of Gaussian white noise or salt pepper noise [1]. The stray light from Moon, Earth, or Sun causes additional interference in the form of uneven background. These interferences are perceived as false or missing stars by the star trackers. Consequently, different image segmentation methods have been employed to acquire stars from digital images contaminated with noise.

Thresholding algorithms are prominent approach to detect stars in a noisy background of the space images. Two different approaches are adopted. The first approach involves calculating a global threshold value and using it for the entire digital image. Nonetheless, global thresholding is only effective if the star gray levels and background are explicitly distinguished [2, 3]. In cases where the background is locally variable under the influence of noise and stray light, applying adaptive thresholding techniques is more useful [4]. However, adaptive thresholding techniques have also been criticized to be either ineffective in suppressing noise or removing interference [5]. Star segmentation is still an active research topic, and recently, new denoising algorithms based on K-means clustering, wavelet transformations, deep learning, and neural networks are proposed [6–10].

### Corresponding author:

Nevsan Sengil

### E-mail:

nsengil@thk.edu.tr

**Received:** March 6, 2022

**Revised:** May 3, 2022

**Accepted:** May 28, 2022

**Publication Date:** September 15, 2022

**DOI:** 10.5152/electrica.2022.22032



Content of this journal is licensed under a Creative Commons Attribution-NonCommercial 4.0 International License.

Thresholding methods are widely used for image segmentation tasks because these methods are both easy to implement and computationally efficient. However, thresholding methods can fall short if the image is highly contaminated with noise. This study is intended to improve the shortcomings of thresholding algorithms in case of heavy interference. Once passed through the optical unit of the star tracker, starlight spreads out in the form of a point spread function (PSF). Star images resemble an elliptical shape and their magnitude decreases radially. Investigations are concentrated on how to distinguish real stars from the noisy background, taking advantage of this unique geometric form.

Density-based spatial clustering of applications with noise (DBSCAN), which is a subset of the machine learning method, is found to be a very efficient technique to accomplish this task. As a result, a hybrid image segmentation method comprising global thresholding and DBSCAN methods is developed. Additionally, a sorting algorithm is added to list and display the required number of brightest stars to increase the efficiency of the star identification algorithm because a limited number of bright stars are sufficient for star identification purposes [11]. For testing, a celestial image originating from a satellite and polluted with different types and levels of noise is used. The first contribution of this article is to improve star detection capabilities of the global thresholding method in the highly noisy background using DBSCAN. Secondly, detected stars are sorted in relation to their brightness to increase the efficiency of the star identification algorithm. The test results show that the proposed hybrid method performed better than the conventional thresholding methods for segmenting heavily polluted images. Furthermore, stars are successfully listed in terms of their brightness.

Following the introduction section, a summary is added to explain main units of the star trackers and their working principles. Next, some brief information is presented about DBSCAN which is subset of machine learning clustering method. The fourth section is devoted to proposed hybrid image segmentation method. In this part, how to calculate thresholds, assign pixel labels, implement DBSCAN, and sort stars are explained in detail. In the next section, proposed and conventional methods are tested and compared in terms of denoising efficiency and computation times. Finally, conclusions and recommended future studies are presented in the last section.

## II. STAR TRACKERS

A generic star tracker is simply composed of an optical lens system, a two-dimensional detector comprising semiconductor sensors, different algorithms run on the processor unit, and a catalog of guide stars. The optical lens system is placed in front of the digital camera. The average number of stars observed by the camera is limited by the field of view (FOV) of the optical lens system, as shown in Fig. 1.

The light photons collected by this lens system are directed to the detector unit. The detector unit contains a two-dimensional charge-coupled device or complementary metal oxide semiconductor (CMOS) pixel sensors. The size of the detector is a function of both the focal length and FOV angle of the optical lens system. Pixel sensors on the detector convert incoming light energy into electronic signals. These electronic signals, also called digital images, contain spatial, radiometric, spectral, and temporal information about the stars.

The processor unit using image segmentation algorithms picks up the stars from the celestial image captured by the star tracker's digital camera. The output of the image segmentation unit includes not only star positions but also radiometric values. A centroiding algorithm calculates the exact coordinates of the star centers using the information coming from the image segmentation unit. These data are forwarded to star identification algorithms. Two different paradigms, either geometric- or pattern-based, are adopted in the star identification algorithms [12]. The former algorithm is also called the angular method. First, three or four stars are chosen from the digital image. Subsequently, the angular distances between these stars and angles between the vertices are calculated and then compared with the star catalog. The latter method is called pattern matching. In this method, a pattern is formed for selected stars from the image, and this pattern is compared to the patterns of the stars stored in the catalog. Once at least two stars are identified, different algorithms such as Triad and Quest are used to estimate the attitude of spacecraft [13].

## III. DBSCAN METHOD

Density-based spatial clustering of applications with noise is subset of unsupervised machine learning and clustering as shown in Fig. 2. It collects data points in the same or different clusters according to two

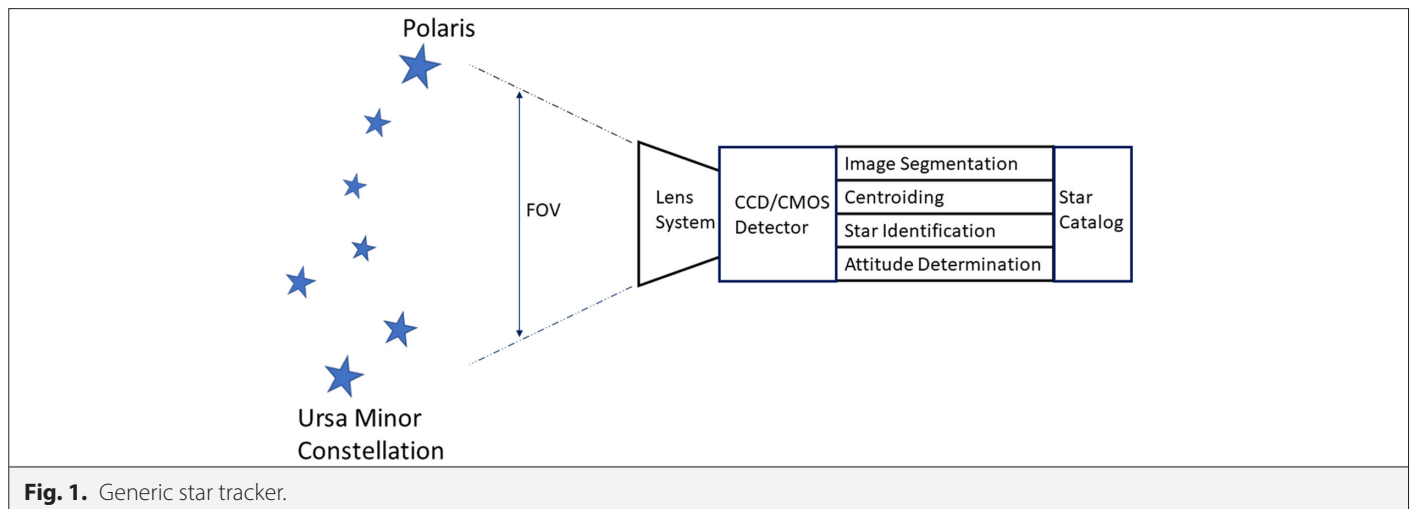
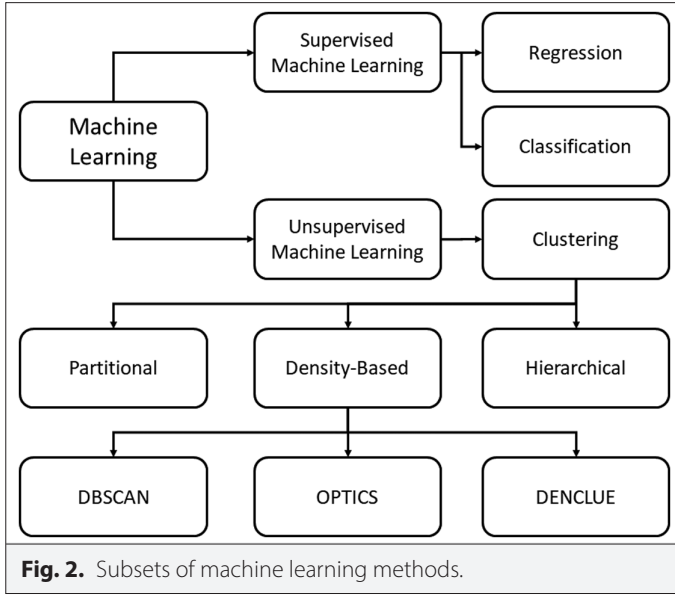


Fig. 1. Generic star tracker.



criteria: length scale ( $\epsilon$ ) and minimum number of points ( $N_{\min}$ ). Two data points are admitted as neighbors if the distance between these points is smaller than  $\epsilon$ . Moreover, a new cluster is formed if the number of neighboring data point is higher than or equal to  $N_{\min}$ . Data points that do not satisfy DBSCAN criteria are determined as noise and removed from the data set. Consequently, DBSCAN achieved recognition in dealing with data sets tampered with interference. Moreover, DBSCAN does not require a pre-set number of clusters in advance. In addition, DBSCAN can detect clusters of arbitrary shapes and sizes [14]. As a result, DBSCAN is one of the most favored cluster algorithms. One of the main drawbacks of the algorithm is the single scale  $\epsilon$  used to search for structures. However, improved DBSCAN algorithms have been developed to overcome this deficiency by using adaptive  $\epsilon$ -distance [15]. Second, the algorithm complexity of DBSCAN is  $O(n^2)$ . A modified algorithm called grid-based DBSCAN is proposed to scale down the computational load to  $O(n \log(n))$  [16].

#### IV. HYBRID IMAGE SEGMENTATION METHOD

Digital images are usually defined as a two-dimensional function  $f(x,y)$ , where  $x$  and  $y$  are spatial coordinates and  $f$  is the brightness or gray level of the data point. In digital images, both the coordinates and gray levels are digitized. Therefore, a digital image is a

matrix of unsigned integer numbers. In digital images, gray levels are represented by digital numbers (DNs). The dynamic range of DNs was defined as  $2^n$ . In this expression,  $n$  is the number of bits. If DNs comprise 8 bits, the DN values are integer numbers limited to between 0 and 255. Hence, a black and white (B&W) image has only 256 gray levels. However, the light energy magnitude ratios between the bright and faint stars are much larger than this value. To detect a wide range of stars, the lowest and highest threshold values should be cautiously chosen. When the radiometric value is lower than or equal to the lowest threshold, the DN on the digital image is recorded as 0. On the contrary, if this value is higher than or equal to the highest threshold, the DN is recorded as 255. If precise light energy magnitudes are required in the calculations, the bit depth should be increased using more bits.

Digital color images comprise red, green, and blue layers. As a result, each data point can have  $2^{24} = 16\,777\,216$  different colors called true colors [17]. One common method to transform a color image into a B&W image is to use the ITU-R BT.601-7 Formula (1), which is given below [18]. In this equation,  $E'_Y$ ,  $E'_R$ ,  $E'_G$ , and  $E'_B$  are DNs for B&W, red, green, and blue layers.

$$E'_Y = 0.299E'_R + 0.587E'_G + 0.114E'_B \quad (1)$$

The stars are far away from the solar system. Even the closest star system, Alpha Centaury is 4.37 light years away. Hence, stars are assumed to be point sources. However, even if no optical aberration is present, the geometric form of a star is not a point on the digital image. The two-dimensional form of starlight on the focal plane can be described as a PSF which corresponds approximately to a Gaussian distribution [19].  $A$ ,  $r$ , and  $\sigma$  are the amplitude, distance from the star center, and standard deviation, respectively.

$$F_{ps}(r, A, \sigma) = Ae^{-\frac{r^2}{2\sigma^2}} \quad (2)$$

A digital image of Alnilam (HIP26311) positioned 2000 light years away from the solar system is given in Fig. 3(a). Digital numbers of Alnilam start from 255 in the center area and gradually degrade to the background in elliptic form. The image of the Orion star constellation is taken by a star tracker camera of NASA CubeSat named Asteria [20] as shown in Fig. 3(b). The Orion star constellation image contains  $831 \times 985$  pixels in the horizontal and vertical directions, respectively. The bit depth is 8 bits. Consequently, the gray levels are limited to between 0 and 255.

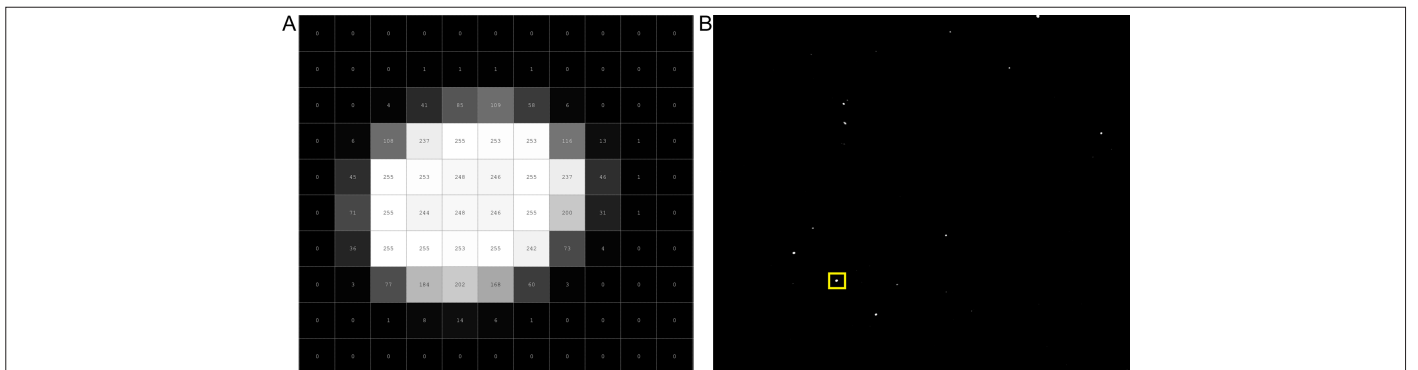


**Fig. 3.** (a) Digital image of Alnilam. (b) Alnilam in Orion star constellation. (courtesy of NASA) [19].

### A. Thresholding Part

A global threshold ( $T_G$ ) is computed as in (3) to separate the background from the foreground [5]. In (3),  $\mu$ , and  $\sigma$  are the mean and standard deviation of the celestial image, respectively.

$$T_G = \mu + 3\sigma \quad (3)$$

### B. Labeling Part

In this part, a new blank image is formed in the memory unit. The size of the celestial image and blank image is equal. To increase the dynamic range, the bit depth of the blank image is designated to be 16 bits.

Consequently, all pixels are revisited on the star image as in Fig. 4(a), and the coordinates of pixels with DNs higher than the threshold value are recorded. Pixels with the same coordinates on the blank image are labeled with a unique integer number as in Fig. 4(b).

### C. DBSCAN Part

In the next step, using the DBSCAN algorithm, the label of neighbor pixels on the empty image is changed to one of the labels, which is still a unique integer number as in Fig. 4(c). The length scale ( $\epsilon$ ) of the DBSCAN is naturally determined as 1 pixel. However, determining the minimum number of points ( $N_{min}$ ) is a more complicated problem. In this study, a stochastic method is suggested. The method begins with a minimum value ( $=2$ ) at the beginning. Over time, the method calculates a new minimum number of points from statistical data obtained from the sorting algorithm.

### D. Sorting Part

Subsequently, all non-zero DNs are counted, and a new one-dimensional histogram is generated. This histogram relates the number of pixels and the brightness level of the stars in the Orion star constellation. This one-dimensional histogram is sorted in

descending order. Hence, the proposed method can easily exhibit both the required number of brightest stars and the rank of their brightness as shown in Fig. 4(d). Alnilam is found to be the fourth brightest star in the given celestial image which is a part of the Orion star constellation. A flow chart of the proposed hybrid image segmentation method is given in Fig. 5.

## V. TESTS AND TEST RESULTS

In the subsequent sections, the celestial image of the Orion constellation taken by Asteria CubeSat is added with Gaussian, salt and pepper, and uneven background noise. Then the developed hybrid image segmentation method which is a combination of both global thresholding and DBSCAN is applied to this noise-added image. Next, the resulting image is compared with the conventional global threshold Otsu's method [21] and adaptive thresholding [22] method. These methods are now implemented in MATLAB as intrinsic functions "graythresh" and "adaptthresh," respectively. First, the resulting images of the proposed hybrid method, Otsu's method, and adaptive thresholding method are displayed for visual inspection. Secondly, these images are compared numerically with the original image in terms of background and foreground pixel values.

Tests are realized on Intel Surface Laptop 2, 8 GB RAM, Intel(R) Core(TM) i5-8250U CPU @ 1.60GHz 1.80 GHz. The operating system is Windows 11.

### A. Adding Noises

Before adding noise, the global threshold, mean, and standard deviation values of the Orion star constellation are calculated and listed as in Table I.

Firstly, sensor-originated noises such as dark current noise, photon shot noise, and switching noise are added to the original Orion

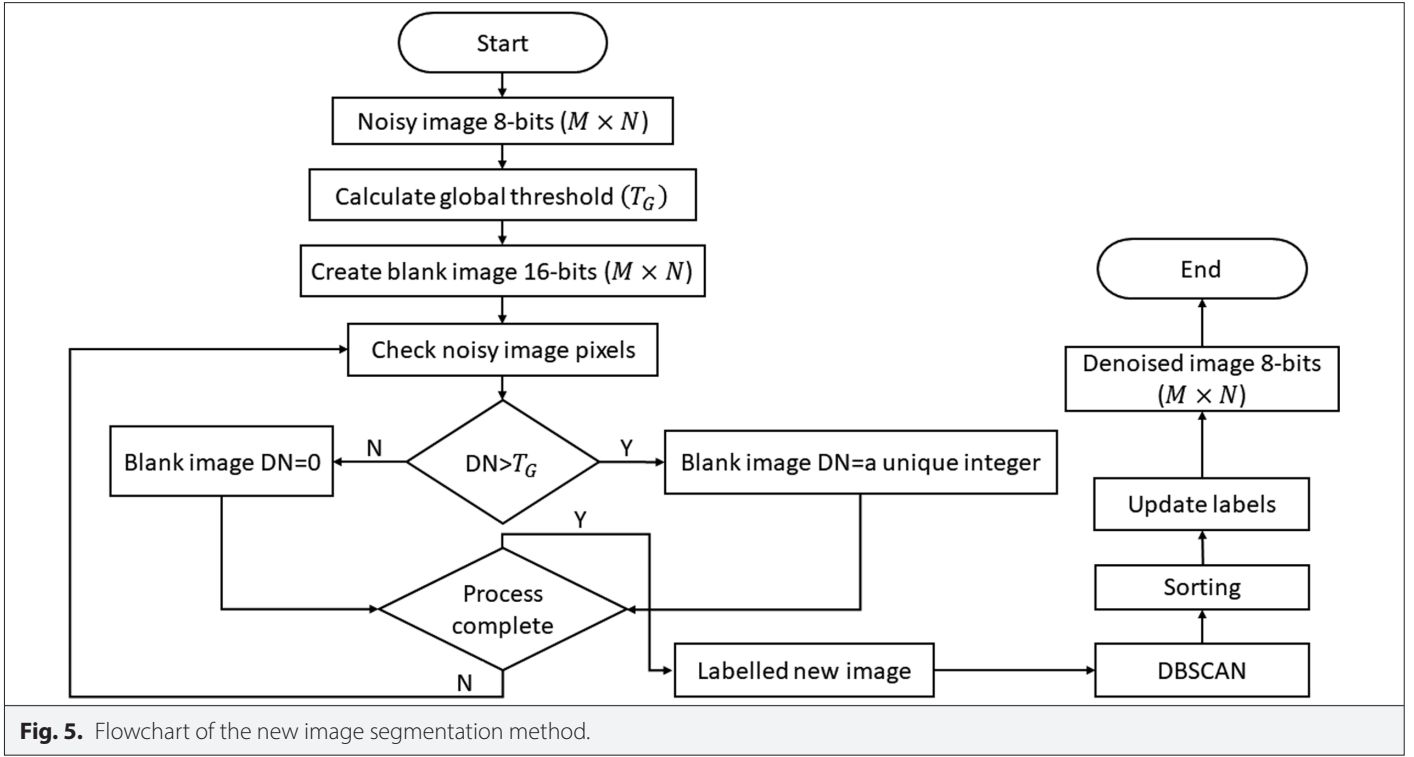
A	291	292	293	294	295	296	297	298	299	300	301
611	0	0	0	0	0	0	0	0	0	0	0
612	0	0	0	1	1	1	1	0	0	0	0
613	0	0	4	41	85	109	58	6	0	0	0
614	0	6	108	237	255	253	253	116	13	1	0
615	0	45	255	253	248	246	255	237	46	1	0
616	0	71	255	244	248	246	255	200	31	1	0
617	0	36	255	255	253	255	242	73	4	0	0
618	0	3	77	184	202	168	60	3	0	0	0
619	0	0	1	8	14	6	1	0	0	0	0
620	0	0	0	0	0	0	0	0	0	0	0

B	291	292	293	294	295	296	297	298	299	300	301
611	0	0	0	0	0	0	0	0	0	0	0
612	0	0	0	0	0	0	0	0	0	0	0
613	0	0	0	385	386	387	388	0	0	0	0
614	0	0	389	390	391	392	393	394	395	0	0
615	0	396	397	398	399	400	401	402	403	0	0
616	0	404	405	406	407	408	409	410	411	0	0
617	0	412	413	414	415	416	417	418	0	0	0
618	0	0	419	420	421	422	423	0	0	0	0
619	0	0	0	424	425	0	0	0	0	0	0
620	0	0	0	0	0	0	0	0	0	0	0

C	291	292	293	294	295	296	297	298	299	300	301
611	0	0	0	0	0	0	0	0	0	0	0
612	0	0	0	0	0	0	0	0	0	0	0
613	0	0	0	385	385	385	385	0	0	0	0
614	0	0	385	385	385	385	385	385	385	0	0
615	0	385	385	385	385	385	385	385	385	0	0
616	0	385	385	385	385	385	385	385	385	0	0
617	0	385	385	385	385	385	385	385	385	0	0
618	0	0	385	385	385	385	385	0	0	0	0
619	0	0	0	385	385	0	0	0	0	0	0
620	0	0	0	0	0	0	0	0	0	0	0

D	291	292	293	294	295	296	297	298	299	300	301
611	0	0	0	0	0	0	0	0	0	0	0
612	0	0	0	0	0	0	0	0	0	0	0
613	0	0	0	4	4	4	4	0	0	0	0
614	0	0	4	4	4	4	4	4	4	0	0
615	0	4	4	4	4	4	4	4	4	0	0
616	0	4	4	4	4	4	4	4	4	0	0
617	0	4	4	4	4	4	4	4	4	0	0
618	0	0	4	4	4	4	4	0	0	0	0
619	0	0	0	4	4	0	0	0	0	0	0
620	0	0	0	0	0	0	0	0	0	0	0

**Fig. 4.** (a) Alnilam's (HIP63503) digital numbers from original image. (b) Blank image pixels are filled with unique integer numbers. (c) DBSCAN image with same unique integer numbers, (d) Alnilam's new labels shows rank of brightness.



constellation image in the form of Gaussian and salt and pepper noises. The mean and variance values of the added Gaussian noise are 0 and 0.001, respectively. The density of the added salt and pepper noise is 0.01. This value is the ratio of the salt and pepper noise added in pixels to the total number of image pixels. Next, stray light noise is added in the form of uneven background. The maximum intensity of the added stray light noise value is 88 [1].

Next, the global threshold, mean, and standard deviation values of the noise-added Orion constellation are calculated and listed in Table II. The global threshold value is increased by 9.6521 times in noisy Orion star constellation image.

#### B. Denoising with Conventional and New Hybrid Methods

First, Otsu's global thresholding method is applied to the noise-added Orion star constellation image. This method is found to be not very effective against an uneven background as seen in Fig. 7(a). Next, the adaptive thresholding method is applied to the same noisy image. Although the uneven background is filtered successfully, many bright pixels in the background are left untouched as in Fig. 7(b). Finally, same image is filtered with the hybrid method.

**TABLE I.** ORION STAR CONSTELLATION IMAGE WITHOUT NOISE

Global Threshold ( $T_G$ )	Mean ( $\mu$ )	Standard Deviation ( $\sigma$ )
10.7876	0.0705	3.5724

**TABLE II.** ORION STAR CONSTELLATION IMAGE WITH NOISE

Global Threshold ( $T_G$ )	Mean ( $\mu$ )	Standard Deviation ( $\sigma$ )
104.2417	26.5526	25.8964

Stars become better discernible and most of the background noise is removed from the image as in Fig. 7(c). Additionally, the brightest 12 stars from the Orion constellation are listed in Fig. 7(d) using sorting property of the hybrid method.

To better justify how effective these applied segmentation methods are, the number of pixels in the foreground and background is calculated and compared in Table III. Additionally, the wall clock time of these methods is also recorded and listed in the same Table III.

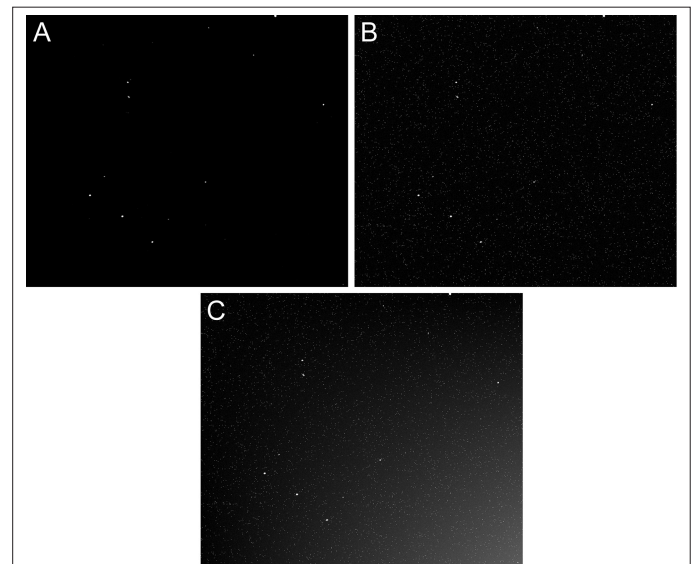


**Fig. 6.** Orion star constellation (a) without noise, (b) Gaussian + pepper and salt noise (c) Gaussian+pepper and salt+uneven background noise. (courtest of NASA) [19].



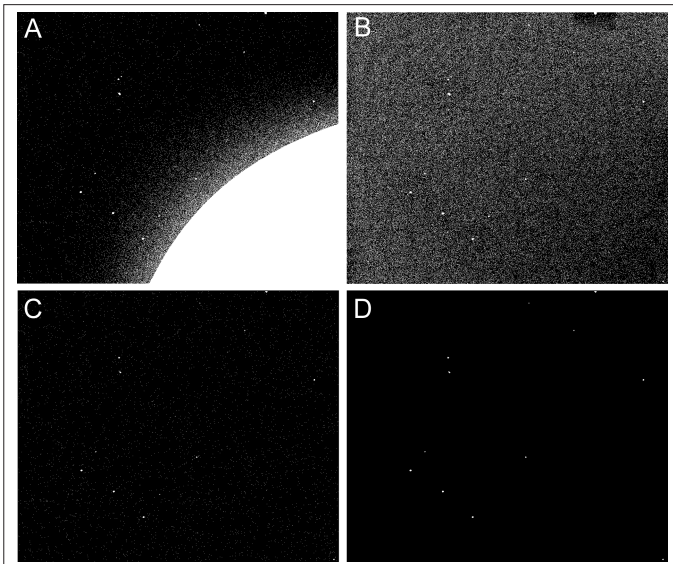


**Fig. 7.** Results of denoising methods. (a) Otsu's global thresholding method, (b) adaptive thresholding method, (c) hybrid method, (d) the brightest 12 stars.

**TABLE III.** FOREGROUND AND BACKGROUND PIXEL NUMBERS

	Foreground Pixels	Background Pixels	Wall Clock Time (s)
Image w/o noise	1330	81 7205	---
Global threshold Otsu's method	216 614	601 921	0.047
Adaptive threshold method	163 880	654 655	0.058
New hybrid method w/o sorting	4203	814 332	0.267

## VI. CONCLUSIONS

Currently, star trackers are the most precise attitude determination sensors. With the advent of technology, these electro-optical devices are more capable and faster than ever. Star trackers are not only the most advanced digital electronic hardware but also robust, error-free methods effective in highly contaminated backgrounds. The focus of this study is on how to better detect stars in heavy interference if conventional algorithms are replaced with a hybrid algorithm which is a combination of both global thresholding and DBSCAN. To date, different types of image segmentation methods based on various paradigms have been developed and employed. Here, a new hybrid image segmentation method is proposed that combines global thresholding, labeling, DBSCAN, and sorting algorithms. For test purposes, Gaussian, salt and pepper, and uneven background noises were added to the Orion star constellation image. The global threshold of the noise added image was increased by 965.21%. Next, a new hybrid method and two other conventional methods were applied to this highly noisy image. Global threshold Otsu's method, adaptive threshold method, and new hybrid method recovered 73.5%, 79.9%, and 99.5% of the background pixels, respectively. Although hybrid method is more complicated and computationally expensive than the conventional

methods, it outperforms these methods in terms of denoising. Shortly, the new hybrid method is less vulnerable to heavy interference stemmed from different type of noises. Additionally, the required number of brightest stars can be displayed instead of all the detected stars. In future studies, it is intended to test the proposed method in star trackers used on CubeSats instead of computer simulations only. Furthermore, proposed method will be compared not only with baseline methods but also with many successful methods developed lately.

**Peer-review:** Externally peer-reviewed.

**Declaration of Interests:** The author have no conflicts of interest to declare.

**Funding:** The author declared that this study has received no financial support.

## REFERENCES

1. Y. He, H. Wang, L. Feng, and S. You, "A novel method of eliminating stray light interference for star sensor," *IEEE Sens. J.*, vol. 20, no. 15, pp. 8586–8596, 2020. [\[CrossRef\]](#)
2. J. Jiang, F. Ji, J. Yan, L. Sun, and X. Wei, "Redundant-coded radial and neighbor star pattern identification algorithm," *IEEE T Aero Elec Sys.*, vol. 4, pp. 2811–2822, 2015. [\[CrossRef\]](#)
3. J. Jiang, L. Lei, and Z. Guangjun, "Robust and accurate star segmentation algorithm based on morphology," *Opt. Eng.*, vol. 55, no. 6, p. 063101, 2016. [\[CrossRef\]](#)
4. M. V. Arbabmir, S. M. Mohammadi, S. Salahshour, and F. Somayehee, "Improving night sky star image processing algorithm for star sensors," *J. Opt. Soc. Am. A Opt. Image Sci. Vis.*, vol. 31, no. 4, pp. 794–801, 2014. [\[CrossRef\]](#)
5. Y. Zou, J. Zhao, Y. Wu, and B. Wang, "Segmenting star images with complex backgrounds based on correlation between objects and 1D Gaussian morphology," *Appl. Sci.*, vol. 11, no. 9, p. 3763, 2021. [\[CrossRef\]](#)
6. A. Khmag, A. R. Ramli, and N. Kamarudin, "Clustering-based natural image denoising using dictionary learning approach in wavelet domain," *Soft Comput.*, vol. 23, no. 17, pp. 8013–8027, 2019. [\[CrossRef\]](#)
7. A. Khmag, A. R. Ramli, S. A. R. Al-haddad, and N. Kamarudin, "Natural image noise level estimation based on local statistics for blind noise reduction," *Vis. Comput.*, vol. 34, no. 4, pp. 575–587, 2018. [\[CrossRef\]](#)
8. X. Liu, L. Song, S. Liu, and Y. Zhang, "A review of Deep-Learning-Based Medical Image Segmentation Methods," *Sustainability*, vol.13, no. 3, 2021. [\[CrossRef\]](#)
9. D. Rijlaarsdam, H. Yous, J. Byrne, D. Oddenino, G. Furano, and D. Moloney, "Efficient star identification using a neural network," *Sensors (Basel)*, vol. 20, no. 13, p. 3684, 2020. [\[CrossRef\]](#)
10. S. Shrimali, A. Pandey, and C. L. Chowdhary, "K-means Clustering-based Radio Neutron Star Pulsar Emission Mechanism," *Rec. Adv. Comp., Sci. Comm.*, vol. 14, no. 1, p. 201-207(7), 2021.
11. C. C. Liebe, "Star trackers for attitude determination," *IEEE Aerosp. Electron. Syst. Mag.*, vol. 10, no. 6, pp. 10–16, 1995. [\[CrossRef\]](#)
12. D. S. Mehta, S. Chen, and K. Low, "A rotation-invariant additive vector sequence based star pattern recognition," *IEEE Trans. Aerosp. Electron. Syst.*, vol. 55, no. 2, pp. 689–705, 2019. [\[CrossRef\]](#)
13. F. L. Markley, and J. L. Crassidis, *Fundamentals of Spacecraft Attitude Determination and Control*. NY, USA: Springer, 2014.
14. G. Lu, and H. Liu, "An effective interference suppression algorithm for visible light communication system based on DBSCAN," *Chin. Opt. Lett.*, vol. 18, no. 1, p. 011001, 2020. [\[CrossRef\]](#)
15. J. H. Kim, J. Choi, K. Yoo, and A. Nasridinov, "AA-DBSCAN: An approximate adaptive DBSCAN for finding clusters with varying densities," *J. Supercomput.*, vol. 75, no. 1, pp. 142–169, 2019. [\[CrossRef\]](#)
16. T. Boonchoo, X. Ao, Y. Liu, W. Zhao, F. Zhuang, and Q. He, "Grid-based DBSCAN: Indexing and inference," *Pattern Recognit.*, vol. 90, pp. 271–284, 2019. [\[CrossRef\]](#)
17. M. Pohanka, "Colorimetric hand-held sensors and biosensors with a small digital camera as signal recorder, a review," *Rev. Anal. Chem.*, vol. 39, no. 1, pp. 20–30, 2020. [\[CrossRef\]](#)

18. *Recommendation ITU-R BT.601-7*, "Studio encoding parameters of digital television for standard 4:3 and wide-screen 16:9 aspect ratios," 2011.
19. H. Wang, Y. Wang, Z. Li, and Z. Song, "Systematic centroid error compensation for the simple Gaussian PSF in an electronic star map simulator," *Chin. J. Aeronaut.*, vol. 27, no. 4, pp. 884–891, 2014. [\[CrossRef\]](#)
20. V. H. Schulz, G. M. Marcelino, L. O. Seman, et al. "Universal verification platform and star simulator for fast star tracker design," *Sensors (Basel)*, vol. 21, no. 3, p. 907, 2021. [\[CrossRef\]](#)
21. N. Otsu, "A threshold selection method from gray-level histograms," *IEEE Trans. Syst. Man Cybern.*, vol. 9, no. 1, pp. 62–66, 1979. [\[CrossRef\]](#)
22. D. Bradley, and G. Roth, "Adapting thresholding using the integral image," *J. Graph. Tool.*, vol. 12, no. 2, pp.13–21, 2007. [\[CrossRef\]](#)



Nevsan Sengil graduated from Control System Engineering in Naval Academy, Turkey, in 1980. He received his M.S. degree in Engineering Science and PhD degree in Astronautical Engineering from Naval Postgraduate School, USA, in 1987 and Istanbul Technical University, in 2008, respectively. He is currently a faculty member at the University of Turkish Aeronautical Association. His studies are focused on rarefied gas dynamics, spacecraft attitude dynamics/control, and flow simulations using particles.